NUMERICAL PREDICTION OF HEAT TRANSFER PHENOMENA FROM A CHIP ASSEMBLY FOR LOW REYNOLDS NUMBER

by

Srinivas G. BHATTA [a*]***, Seetharam T. RAMARAO*** [b]***,***
and Kankanhalli N. SEETHARAMU [b]

[a] Department of Mechanical Engineering, New Horizon College of Engineering, Bangalore, Karnataka, India
[b] Department of Mechanical Engineering, P. E. S. Institute of Technology, Bangalore, Karnataka, India

Original scientific paper
UDC: 621.315.592:519.872:536.24
DOI: 10.2298/TSCI1102379B

A 3-D study of heat transfer from three heated blocks in a square channel at a Reynolds number of 108 with height of the chip assembly as the characteristic length is presented. Heated blocks affixed to the bottom plate represent electronic chips mounted on horizontal circuit board. A hexahedron block is affixed on to the top shrouding wall over the heated section. Thickness of this block is varied to study the effect on heat transfer from the chip assembly. A block of thickness equal to the passage between substrates produces maximum heat transfer enhancement. A block over the first passage enhances heat transfer from both immediate upstream and downstream chips considerably. A block over each recirculation zone produces moderate heat transfer from all the chips for a moderate pressure-drop. It is also observed that addition of blocks in the top plate does not add much to the pressure-drop in the duct.

Keywords: *semiconductor device, heat transfer enhancement, hexahedron blocks, low Reynolds number*

Introduction

Numerical simulation has become a popular tool for investigating thermal characteristics of semiconductors. In the recent electronic packaging design of low power rated electronic components on printed circuit boards, specific consideration is accorded for heat transfer analysis to achieve high dissipation rates. This concern has generated motivation for research study of forced convection cooling in electronic equipments with printed circuit boards. The flow in these channels is usually low due to small dimensions and so, a number of unique methods have been proposed for heat transfer enhancement.

Konecni *et al.* [1] investigated experimentally the influence of the Reynolds number and Grashoff number on the Nusselt number for low inlet velocities. The research group reported that even at low Reynolds numbers, forced convection was the dominant mode of heat transfer wherein natural convection could be neglected. Bhatta *et al.* [2] undertook a numerical investigation and compared with the experimental holographic isothermal fringes of heated chips in a square duct. The authors reported that there was a qualitative and

* Corresponding author; e-mail: gsb.mech@gmail.com

quantitative agreement between the numerical isotherms and experimental isotherms. A unique method of heat transfer enhancement from an array of chips was reported by Ratts *et al.* [3]. The vortices shed from the cylinders were made to provide an internal modulation of the air flow, and the vortices were tuned to the least stable frequency of the system. The investigators noticed that a cylinder above the rear edge of every row of chips provided maximum heat transfer enhancement for low velocities. Experiments were conducted by Sparrow *et al.* [4] to investigate the heat transfer and fluid flow characteristics of arrays of heat generating, block-like modules in a parallel plate channel with flow barriers attached to the bottom plate and in between modules. Forced convection air flow was employed for this purpose. The penalty for enhancement in terms of pressure drop was considerably high, and it was more than five fold. Hung *et al.* [5] investigated experimentally the effect of turbulence promoters affixed to the opposite wall, on heat transfer in a vertical rib heated channel for high inlet velocities. The researchers found that the promoter over the front end of any heated rib, not only enhanced heat transfer performance of its downstream ribs, but also of its upstream ribs. It was reported that greater Nusselt number occurred at the rib immediately downstream of the promoter.

Karniadakis *et al.* [6] studied the influence of flow destabilizers for a wide range of Reynolds number, and it was reported that low Reynolds number flows were optimal with regard to enhancement of heat transfer. Alawadhi [7] performed a two dimensional numerical analysis in a horizontal channel containing heated blocks on the top and bottom plates with a wavy plate in between, and reported that the wavy plate could reduce the temperature of the blocks by maximum of 23%. Sultan [8] conducted experiments to study the forced convection heat transfer in a horizontal channel with multiple protruded heat sources attached to the bottom plate. Perforated holes introduced in the base of the channel in a staggered manner in two rows between heat sources enhanced heat transfer by a maximum of 33%. An experimental investigation was carried out by Chomdee *et al.* [9] to study the heat transfer enhancement by delta winglet vortex generators in air cooling of a staggered array of rectangular electronic modules. It was reported that vortex generators enhanced the adiabatic heat transfer coefficients, and reduced the thermal wake function and module temperatures significantly. A microfin array heat sink using the flow induced vibration of a microfin array was investigated by Go *et al.* [10] to identify its effect on heat transfer enhancement in a laminar flow regime. Based on the dynamics of the microfin vibration and the thermal performance comparison, it was concluded by the investigators that the vibrating deflection of the microfin plays a major role in enhancing the heat transfer rate from the microfin array heat sink.

The present 3-D numerical investigation predicts heat transfer characteristics of three heated chips with and without the turbulence promoters affixed to the top plate of a square channel. The authors have not come across in the literature any investigation involving the geometric positioning of turbulence promoters affixed to the top shrouding wall in a horizontal square duct with chip-like heated modules for low Reynolds number. The present study encompasses the effect of positioning, number, and thickness of hexahedron blocks attached to the top shrouding wall, on heat transfer from the chips and the static pressure-drop in the channel.

Analysis

The geometry and nomenclature of the calculation domain are depicted in fig. 1, which approximates the cross-sectional views of the chip assembly in Konecni *et al.* [1]. The

apparatus consists of a small wind tunnel 200 mm long with 25 × 25 mm^2 cross-section. The bottom surface of the tunnel is lined with a layer of teflon and a circuit board is placed over it. Three IC chips provide the heating surfaces. The chip dimensions are 21.5 × 6.4 × 2 mm^3. Each chip is mounted on a Bakelite substrate of 21.5 × 8 × 6 mm^3 dimensions. From here onwards, an assembly of a chip and a substrate is addressed as a chip assembly or just a chip. Figure 2 shows the grid distribution in the calculation domain. Dense grids are generated closed to the walls to span the laminar sublayer. Non-staggered, non-uniform grids are employed in FLUENT with the QUICK scheme to interpolate the grid stored velocities to the interfaces, and hexahedron cells fill the entire domain.

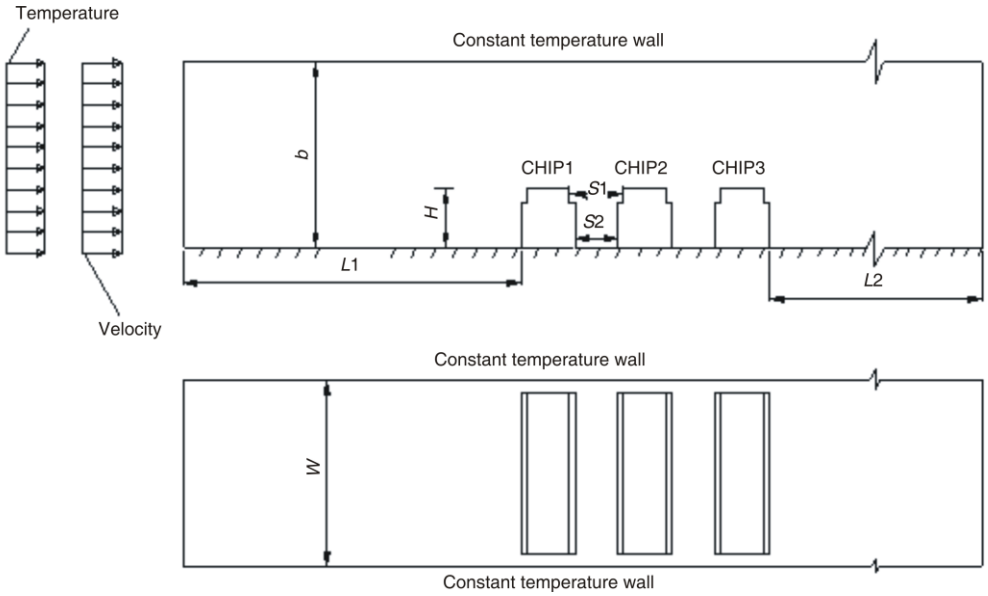

Figure 1. Geometry, nomenclature, and some boundary conditions of the calculation domain, H = 8 mm, $L1$ = 50 mm, $L2$ = 114 mm, $S1$ = 8 mm, $S2$ = 6.4 mm, b = W = 25 mm

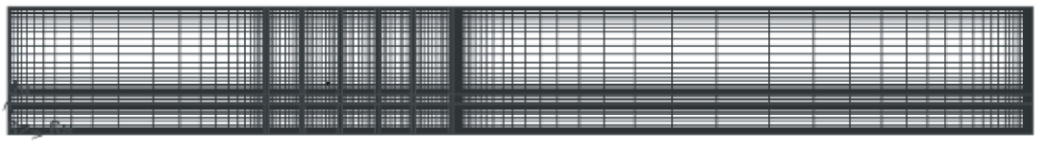

Figure 2. Grid distribution in X-Y directions showing dense grids near the walls, inlet, and exit

Three dimensional continuity, momentum, and energy equations are considered for the calculation purpose. The k-ε model is chosen as an eddy viscosity model to account for the effect of turbulence. Thermo-physical properties of air, except for density, are assumed to be constant. Though small, the effect of natural convection is incorporated by providing information of fluid density as function of temperature and gravitational acceleration in the downward direction normal to the flow. The discrete transfer radiation model (DTRM) of Carvalho *et al.* [11] is included in all the calculations to account for the radiation effect. The DTRM, here in this calculation, assumes gray radiation with the predicted radiant intensity representing an integrated one across all wave lengths.

Boundary conditions

Inlet air velocity and temperature profiles are assumed to be uniform since a flow straighter is employed at the inlet of the test section. Pressure boundary condition is imposed at the outlet as the test section is not long enough to assume that the flow is fully developed at the outlet. Constant temperature boundary condition is assumed at the surface of the chip assembly because the average thermal conductivity of the material of the chip assembly, which is 0.262 W/mK, is nearly ten times the thermal conductivity of air at the inlet. The turbulent intensity at the inlet and exit of the channel are taken uniformly to be 10% for the turbulent flow. The velocity components along all solid boundaries are zero. The temperature along the top and side plates of the channel is measured to be equal to the room temperature, and the bottom teflon coated plate is assumed to be adiabatic. Air does not participate in the radiation exchange process as absorption and scattering coefficients of air are assumed to be negligible. The emissivity of the chip and socket assembly is taken to be 0.9.

Solution technique

Linearized continuity, momentum, energy, turbulent kinetic energy, and turbulent diffusivity equations give rise to seven variables: u, v, w, h, k, ε, and p. The equations are solved sequentially using the FLUENT code which supports the SIMPLE algorithm. Line-by--line technique coupled with the Gaussian elimination method is used to solve the tridiagonal matrices obtained by algebraic equations for all the variables. Block correction, one dimensional correction to the enthalpy field for the over all heat transfer balance, is applied to enthalpy equations to expedite the convergence. Pressure and enthalpy equations are swept 20 times in all the iterations. Convergence is declared when the difference in successive iteration values of all the variables are less than 10^{-6}.

Results and discussion

Numerically predicted values are validated with the experimentally obtained ones as explained in Bhatta *et al*. [2]. They agree reasonably well with each other. A grid independent solution is reached when three different maximum grid sizes (2 mm, 1.6 mm, 1.2 mm) are adopted for the basic geometrical configuration without the turbulence promoters. The corresponding total numbers of grid cells are 37530, 43113, and 60057, respectively. Grid independent solution is declared when maximum changes in average Nusselt numbers for all the heated surfaces are less than 1% for the successive grid sizes. Computations are carried out for inlet velocity corresponding to the Reynolds number as low as 108, with height of the chip assembly as the characteristic length.

The heat transfer and flow characteristics of the domain are investigated for the following cases: (1) the thickness of a hexahedron block in the x-direction is varied in the range of 0.25 to 1.0 of S_2 keeping the width and height constant, (2) the geometrical location of the block is varied for eleven discrete locations as shown in fig. 4, (3) two blocks are employed with a varying gap in between, and (4) a block is installed over each recirculation zone created behind each chip. In all these cases, the height and width of the blocks are taken to be same as that of the chip.

Heat transfer from the chip is quantified by average Nusselt number, and that is calculated by:

$$\overline{\mathrm{Nu}} = \frac{\bar{h}H}{K_{\mathrm{air}}} \tag{1}$$

Here, H = 8 mm is the height of the chip assembly. The average heat transfer coefficient, $\bar{h}$ is obtained by:

$$\bar{h} = \frac{1}{A_s \Delta T} \int_{A_s} q'' \mathrm{d}A_s \tag{2}$$

where q'' is the local heat flux at the chip surface in W/m^2, A_s – the heated surface area of the chip assembly, dA_s – the area of each cell parallel to the chip surface, and

$$\Delta T = T_c - T_{bm} \tag{3}$$

where T_c is the chip temperature, and T_{bm} – the mean bulk temperature calculated by involving the inlet bulk temperature, T_{bi}, and the exit bulk temperature, T_{bo}. for each chip assembly as:

$$T_{bm} = \frac{T_{bi} + T_{bo}}{2} \tag{4}$$

The exit bulk temperature of the fluid for each chip is calculated by the relation:

$$T_{bo} = T_{bi} + \frac{\int_{A_s} q'' \mathrm{d}A_s}{\rho U A C} \tag{5}$$

It is to be noted that the inlet air temperature is the inlet bulk temperature for chip 1 and the exit bulk temperature of the first chip becomes the inlet bulk temperature for the second chip, and so on.

Figure 3 shows the average Nusselt number of each chip for different dimensionless thicknesses of the hexahedron block affixed to the top plate of the square channel over the recirculation zone produced behind the first chip. It is imperative from the graph that heat transfer from all the chips increases for thickness beyond 0.5 for obvious reason of increased turbulence. But, there is an aberration in the behavior of the average Nusselt number curve from 0.2 to 0.5 thicknesses. In this region, as the block width increases, for chip 1 and 3, not much heat transfer improvement is noticed. Although, there is a decrease in heat transfer in this range for chip 2, and this behavior could be attributed to the reason that the flow is by-passed away from chip 2 for the said thickness range as evident from the velocity plot. Average Nusselt numbers for all the chips are depicted in the same figure for no-block condition at ΔX = 0. An increasing trend of average Nusselt number is observed even for a block thickness of ΔX = 1.

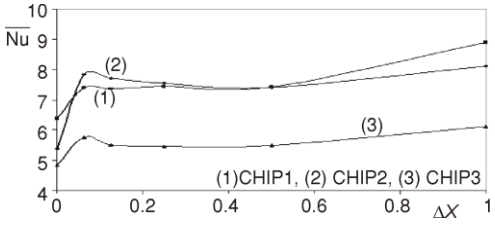

Figure 3. Heat transfer from chips with variation of dimensionless block thickness, $\Delta X = t/S2$

In the second section of the study, a hexahedron block with thickness equal to S_2 (ΔX = 1) is introduced in the domain, and it is moved from the initial position over the front edge of the first chip, to the final position over the rear edge of the last chip as shown in fig. 4.

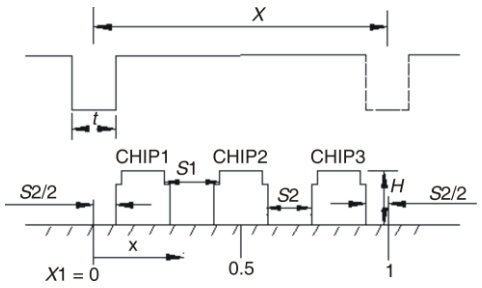

Figure 4. Arrangement of a block over the chips, dimensionless distance, *X*1 = *x*/*X*

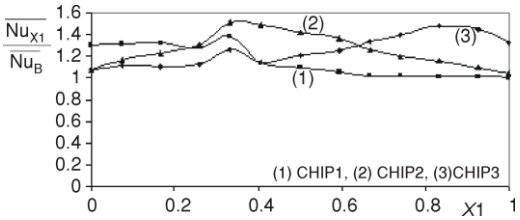

Figure 5. Heat transfer behavior of chips with variation of *X*1 from 0 to 1 with reference to fig. 4

Here, the block's position refers to the centerline of the block in the streamwise direction. Heat transfer from the chips and pressure-drop in the channel are calculated for each location of the block. Figure 5 indicates the heat transfer enhancement for each chip for discrete locations of one block, while the configuration of no-block serves as the reference for comparison of heat transfer enhancement. Maximum heat transfer is obtained from chips 1 and 2 when the block is positioned right above the recirculation zone formed behind chip 1. For this configuration, chip 1and chip 2 experience 39% and 51% improvement in heat transfer, respectively. Average Nusselt numbers of all the chips are nearly equal when the block's centerline is just above the front edge of the last chip, *i. e.*, *X*1 position of 0.74. Average Nusselt number of each chip and percentage heat transfer improvement for different block locations starting from 0 to 1 are shown in tab. 1. Third chip experiences a maximum of 48% improvement in heat transfer when the block is just right above it. The considerable increase in heat transfer from chips 1 and 2 is attributed to increased recirculation strength behind chip 1, due to the introduction of the block over the chip assembly as shown in fig. 6 and fig. 7.

Table 1. Average Nusselt numbers of the chips with one block; values in parentheses indicate % heat transfer enhancement

Dimensionless distance, *X*1 (refer to fig. 4)	$\overline{\mathrm{Nu}}_{\mathrm{chip1}}$	$\overline{\mathrm{Nu}}_{\mathrm{chip2}}$	$\overline{\mathrm{Nu}}_{\mathrm{chip3}}$
0.0	8.37 (31.0)	5.80 (8.0)	5.24(8.5)
0.074	8.45 (32.0)	6.29 (17.0)	5.41 (12.0)
0.167	8.50 (33.0)	6.63 (23.5)	5.34 (10.5)
0.259	8.23 (28.8)	7.00 (30.4)	5.44 (12.6)
0.333 (block over recirculation zone formed between chip 1 and chip2)	8.89 (39.0)	8.12 (51.2)	6.11 (26.5)
0.407	7.28 (13.9)	8.04 (49.7)	5.64 (15.0)
0.5	7.00 (9.5)	7.66 (42.6)	5.87 (21.5)
0.593	6.77 (6.0)	7.34 (36.7)	6.07 (25.7)
0.667	6.57 (2.8)	6.80 (26.6)	6.46 (33.7)
0.74	6.57 (2.8)	6.47 (20.5)	6.79 (40.6)
0.833	6.51 (1.9)	6.22 (15.8)	7.16 (48.2)
0.926	6.49 (1.8)	5.90 (9.9)	7.00 (44.9)
1.0	6.40 (0.2)	5.63 (4.8)	6.42 (32.9)

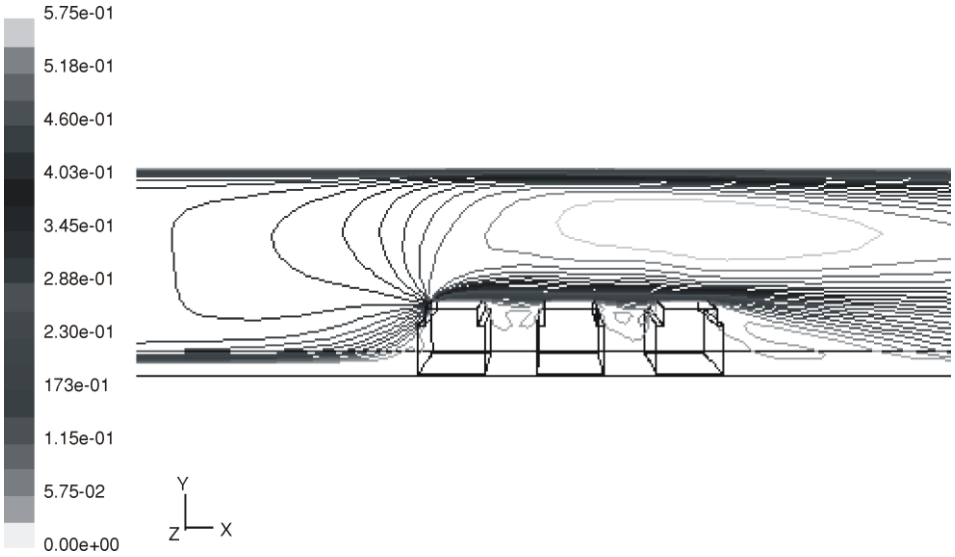

Figure 6. Velocity contours without block in X-Y directions at the centre of Z

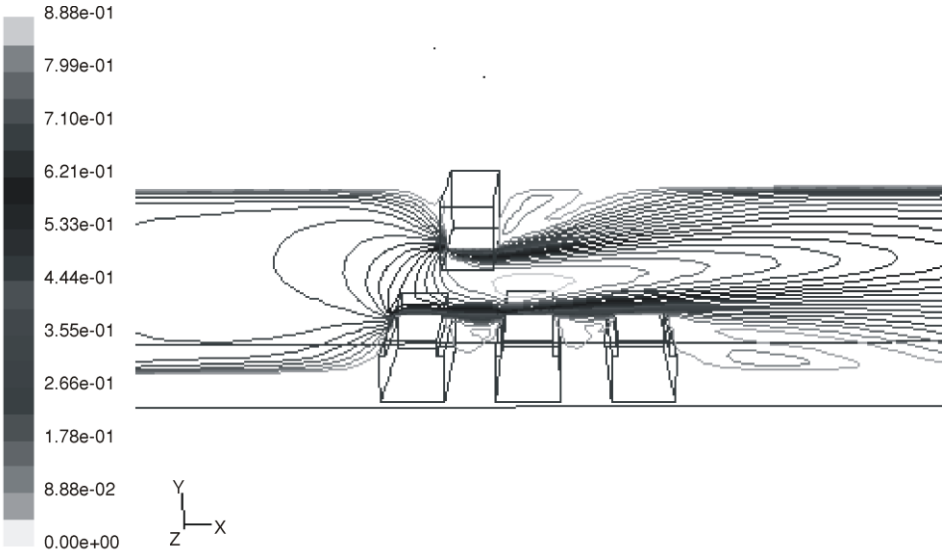

Figure 7. Velocity contours when the block of thickness S_2 is over the recirculation zone formed behind first chip

Further analysis is carried out by introducing two blocks at a distance. One block is stationed over first recirculation zone in this entire analysis, because this configuration produces maximum heat transfer from chips 1 and 2. The second block is moved discretely along the top shrouding wall from 0 to 1 as shown in fig. 8. Here, 0 and 1 indicate the initial and final positions of the second block, while the first block is unmoved. Figure 9 shows the heat transfer improvement from each chip, when the basic no-block configuration serves as

the reference for the calculation of heat transfer enhancement. Variations of heat transfer from all the three chips are evident when the second block moves from 0-position to 0.5-position. But, the variation of heat transfer improvement is almost nonexistent beyond 0.5-position. When the second block is at X2 position of 0.222, *i. e.*, over the front edge of chip 3 referring to tab. 2, maximum heat transfer improvement occurs for the third chip.

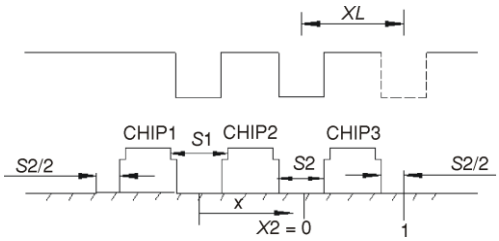

Figure 8. Arrangement of two blocks with a gap in between, $X2 = (x - XL)/XL$

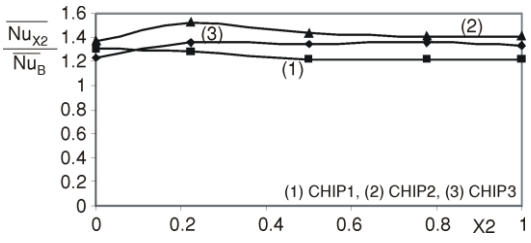

Figure 9. Heat transfer behavior of chips with variation of *X*2 from 0 to 1 as shown in fig. 7

Table 2. Average Nusselt numbers of the chips with two blocks; values in parentheses indicate % heat transfer enhancement

Dimensionless distance, *X*2 (refer to fig. 7)	$\overline{Nu}_{chip1}$	$\overline{Nu}_{chip2}$	$\overline{Nu}_{chip3}$
0.000	8.38 (31.1)	7.36 (37.1)	5.96 (23.4)
0.222 (second block over front edge of the chip 3)	8.14 (27.4)	8.15 (51.8)	6.58 (36.2)
0.500	7.80 (22.0)	7.74 (44.0)	6.51 (34.8)
0.778	7.78 (21.7)	7.58 (41.1)	6.56 (35.8)
1.000	7.73 (21.0)	7.54 (40.4)	6.45 (33.5)

The heat transfer from the middle chip is almost unaffected by the introduction of the second block. The second block proves detrimental for heat transfer enhancement from the first chip as there is a reduction of heat transfer of 12% for *X*2 position of 0.222 due to possible reason that the main flow deviates away from the recirculation zone formed behind chip 1. A block over each recirculation zone provides 21%, 45%, and 33% heat transfer improvement from chip 1, chip 2, and chip 3, respectively, compared to the values of no-block configuration.

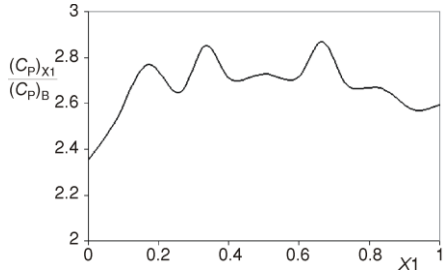

Figure 10. Pressure coefficient ratios for different *X*1 with one-block configuration

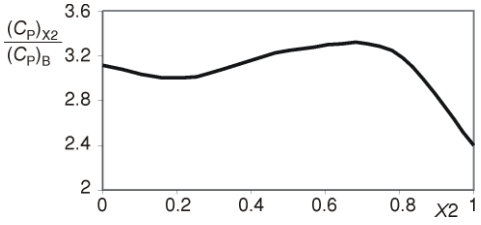

Figure 11. Pressure coefficient ratio *vs.* *X*2 for two-block configuration

The heat transfer enhancement comes with a penalty in terms of increased pressure--drop. A block in the top plate over the test section increases the pressure-drop by an average of 2.7 times compared to that of no-block configuration as shown in fig. 10. As evident from fig. 11, the introduction of one more block at a distance does not add much to the pressure-drop, and the value decreases for the increased gap between the blocks. A block over each recirculation zone produces a pressure coefficient of 2.56, which is less than the value for one-block configuration of maximum heat transfer.

Conclusions

A hexahedron block in the spanwise direction attached to the top shrouding wall of a square channel and placed over the recirculation zone formed behind the first chip enhances heat transfer from both the immediate upstream and downstream chips considerably. The last chip experiences maximum heat transfer when the block is right over the same chip. All the three chips dissipate nearly the same amount of heat for the configuration that the block is placed over the front edge of the last chip. Second block in the top plate, placed at a distance from the first, does not contribute much in the heat transfer enhancement from the middle chip. This arrangement proves beneficial for the last chip, and the same configuration is detrimental for the first chip. A block over recirculation zone formed behind the first chip produces more heat transfer from the first and the middle chips than the configuration that contains a block over each recirculation zone.

There is a 2.8-fold increase in pressure-drop for maximum heat transfer by the introduction of a block in the top shrouding wall of the duct. Additional blocks do not add much to the pressure-drop, and the value decreases as the gap between the blocks increases.

Nomenclature

A – cross-sectional area of the duct, [m^2]
b – height of the channel, [m]
C – specific heat of air, [Jkg^{-1}K^{-1}]
C_P – pressure coefficient, $\Delta P/(1/2\rho U^2)$
$(C_P)_B$ – pressure coefficient in the duct with no--block configuration (reference configuration)
$(C_P)_{X1}$ – pressure coefficient in the duct with one-block configuration
$(C_P)_{X2}$ – pressure coefficient in the duct with two-block configuration
H – height of the chip assembly, [m]
h – average heat transfer coefficient, [Wm^{-2}K^{-1}]
K_{air} – thermal conductivity of air, [Wm^{-1}K^{-1}]
$\overline{Nu}$ – avegage Nusselt number of a chip
$\overline{Nu}_B$ – average Nusselt number of a chip for no-block configuration
$\overline{Nu}_{X1}$ – average Nusselt number of a chip for one-block configuration
$\overline{Nu}_{X2}$ – average Nusselt number of a chip for two-block configuration
$\overline{Nu}_{chip1}$ – average Nusselt number of chip 1
$\overline{Nu}_{chip2}$ – average Nusselt number of chip 2
$\overline{Nu}_{chip3}$ – average Nusselt number of chip 3
ΔP – static pressure drop between inlet and outlet of the duct, [Pa]
Re – Reynolds number, (= UH/ν)
$S1$ – space between chips in streamwise direction, [m]
$S2$ – space between substrates in streamwise direction, [m]
t – thickness of the block, [m]
U – inlet mean velocity, [ms^{-1}]
w – width of the duct, [m]
X – position of hexahedron block, see fig. 4
ΔX – dimensionless thickness of the block, t/S2
XL – position of second block, see fig. 8
$X1$ – dimensionless distance, see fig. 4
$X2$ – dimensionless distance between blocks, $X2 = (x - XL)/XL$, see fig. 8

References

[1] Konecni, S., *et al.*, Convection Cooling of Microelectronic Chips, *Proceedings*, Inter-Society Conference on Thermal Phenomena in Electronic Systems, I-THERM III, Austin, Tex., USA, 1992, pp. 138-144

[2] Bhatta, S. G., *et al*., Numerical Prediction of Heat Transfer in Semiconductor Devices, *ASME Journal of Advances in Electronic Packaging*, *42* (1993), 2, pp. 782-788
[3] Ratts, E., *et al*., Cooling Enhancement of Forced Convection Air Cooled Chip Array through Flow Modulation Induced by Vortex Shedding Cylinders in Cross Flow, Cooling Technology for Electronic Equipment, Hemisphere Publ. Comp., Washington D. C., USA, 1988
[4] Sparrow, E. M., Vemuri, S. B., Kadle, D. S., Enhanced and Local Heat Transfer, Pressure-Drop, and Flow Visualization for Arrays of Block-Like Electronic Components, *International Journal of Heat and Mass Transfer*, *26* (1983), 5, pp. 689-699
[5] Hung, Y. H., Lin, H. H., An Effective Installation of Turbulence Promoters for Heat Transfer Augmentation in a Vertical Rib Heated Channel, *International Journal of Heat and Mass Transfer*, *35* (1992), 1, pp. 29-42
[6] Karniadakis, G. E., Mikic, B. B., Patera, A. T., Heat Transfer Enhancement by Flow Destabilization: Application to the Cooling of Chips, Cooling Technology for Electronic Equipment, Hemisphere, Publ. Comp., Washington D. C., USA, 1988
[7] Alawadhi, E. M., Forced Convection Cooling Enhancement for Rectangular Blocks Using a Wavy Plate, *IEEE Transactions on Components and Packaging Technologies*, *28* (2005), 3, pp. 525-533
[8] Sultan, G. I., Enhancing Forced Convection from Multiple Protruding Heat Sources Simulating Electronic Components in a Horizontal Channel by Passive Cooling, *Microelectronics Journal*, *31* (2000), 9, pp. 773-779
[9] Chomdee, S., Kiatsiriroat, T., Enhancement of Air Cooling in Staggered Array of Electronic Modules by Integrating Delta Winglet Vortex Generators, *International Communication in Heat and Mass Transfer*, *33* (2006), 5, pp. 618-626
[10] Go, J. S., *et al*., Heat Transfer Enhancement Using Flow Induced Vibration of a Microfin Array, *Sensors and Actuators A: Physical*, *90* (2008), 3, pp. 232-239
[11] Carvalho, M. G., Farias, T., Fontes, P., Predicting Radiative Heat Transfer in Absorbing, Emitting, and Scattering Media Using the Discrete Transfer Method, *Fundamentals of Radiation Heat Transfer*, *ASME HTD*, *160* (1991), 1, pp. 17-26

Paper submitted: May 14, 2009
Paper revised: March 16, 2010
Paper accepted: September 23, 2010